

## Responsive plasma polymerized ultrathin nanocomposite films

Kyle D. Anderson<sup>a</sup>, Robert B. Weber<sup>a</sup>, Michael E. McConney<sup>b</sup>, Hao Jiang<sup>b</sup>, Timothy J. Bunning<sup>b</sup>, Vladimir V. Tsukruk<sup>a,\*</sup>

<sup>a</sup>School of Materials Science and Engineering, Georgia Institute of Technology, Atlanta, GA 30332, United States

<sup>b</sup>Materials and Manufacturing Directorate, Air Force Research Laboratory, Wright-Patterson Air Force Base, Dayton, OH 45433-7702, United States

### ARTICLE INFO

#### Article history:

Received 28 May 2012

Received in revised form

27 July 2012

Accepted 4 August 2012

Available online 21 August 2012

#### Keywords:

NIPAAm

Plasma polymerization

Co-polymerization

Responsive films

Tunable optical properties

### ABSTRACT

The plasma polymerization of NIPAAm and titanium isopropoxide monomers into responsive ultrathin films with responsive optical properties using plasma enhanced chemical vapor deposition is reported. The composite ultrathin films possess a large window for potential changes in their refractive index from 1.60 to 1.95. We demonstrated that these polymer films exhibit fast (transition time below 2 s), large, reversible, and repeatable changes to their thickness and refractive index as a function of periodic environmental humidity changes.

© 2012 Elsevier Ltd. All rights reserved.

### 1. Introduction

Material coatings capable of autonomous, self-actuating response to specific stimuli are desirable in a wide range of applications including thermal and chemical sensing, tunable optics, targeted drug delivery, switchable surfaces and micro actuators [1–6]. Designing materials which are capable of generating a response from the stimulus itself eliminates the need for additional and complex triggering and control mechanisms as the response process will be fully contained within a layer of material integrated into the larger system. Responsive ultrathin polymeric films have been utilized in an array of applications through a variety of synthesis methods and materials. Polymers including poly(*n*-isopropylacrylamide) (pNIPAAm) exhibit a large response to temperature in a fluid environment, typically as a change in thickness for thin films, under appropriate conditions as has been widely reported [7–11]. Recent examples include coatings fabricated with UV-photografting and chemical vapor deposition (CVD) techniques [12–16]. This type of switching behavior can be used to drive mechanical changes in systems, actuate folding behavior, alter surface mechanical properties or enhance switchable cell scaffoldings [17–20].

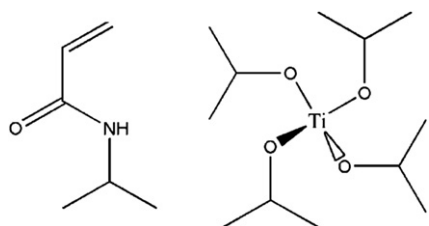
Plasma enhanced chemical vapor deposition (PECVD) polymerization is a unique thin film fabrication method which allows

the direct deposition and polymerization of a wide variety of monomers directly on a target substrate through a one step, robust, solvent-less deposition process [21,22]. PECVD typically utilizes an RF plasma in a low pressure argon atmosphere to radicalize monomer vapor in the plasma stream. PECVD helps to overcome limitations in wet chemical surface modification including challenges with grafting and polymerization while providing a method to precisely control the optical properties of the deposited film. Similar to other CVD techniques, this variant has been utilized for use with organic monomers to enable the formation of a variety of atypical polymers deposited directly onto various planar, freely suspending, and textured substrates for numerous surface modification applications [23–28]. The range of precursors has covered many traditional reactive monomers such as styrene, ethylene glycol and benzene, as well as responsive materials like 2-hydroxyethyl methacrylate, 2-vinylpyridine and *n*-isopropylacrylamide and biological monomers such as amino acids [29–35]. PECVD allows deposition under “dry” conditions meaning that only the pure monomer and no additional solvents, surfactants or reactants are needed in the synthesis of the film. This approach becomes especially useful for the fabrication of robust coatings which may otherwise require complex wet chemical procedures to firmly attach to some surfaces.

A number of recent studies have exploited pNIPAAm as a plasma polymerizable material which retains its well-known and characteristic temperature and humidity response properties [12,33,34].

\* Corresponding author. Tel.: +1 404 894 6081; fax: +1 404 385 3112.

E-mail address: vladimir@mse.gatech.edu (V.V. Tsukruk).



**Scheme 1.** NIPAAm (left) and TTIP (right) monomers used in plasma polymerizations.

Hess et al. conducted extensive temperature and pressure experiments and related changes of the crosslinking properties as measured via FTIR and contact angle measurements back to the reactor conditions [34]. These observations indicate a similar low critical solution temperature (LCST) phase transition and swelling properties of these plasma polymerized materials to bulk materials [33]. Ratner et al. investigated the LCST effects in plasma polymerized NIPAAm using AFM mechanical data measurements as a function of temperature [12,36]. Gleason et al. recently demonstrated the ability to control the LCST between 16 and 28 °C [37]. This was achieved by varying the amount of co-monomer

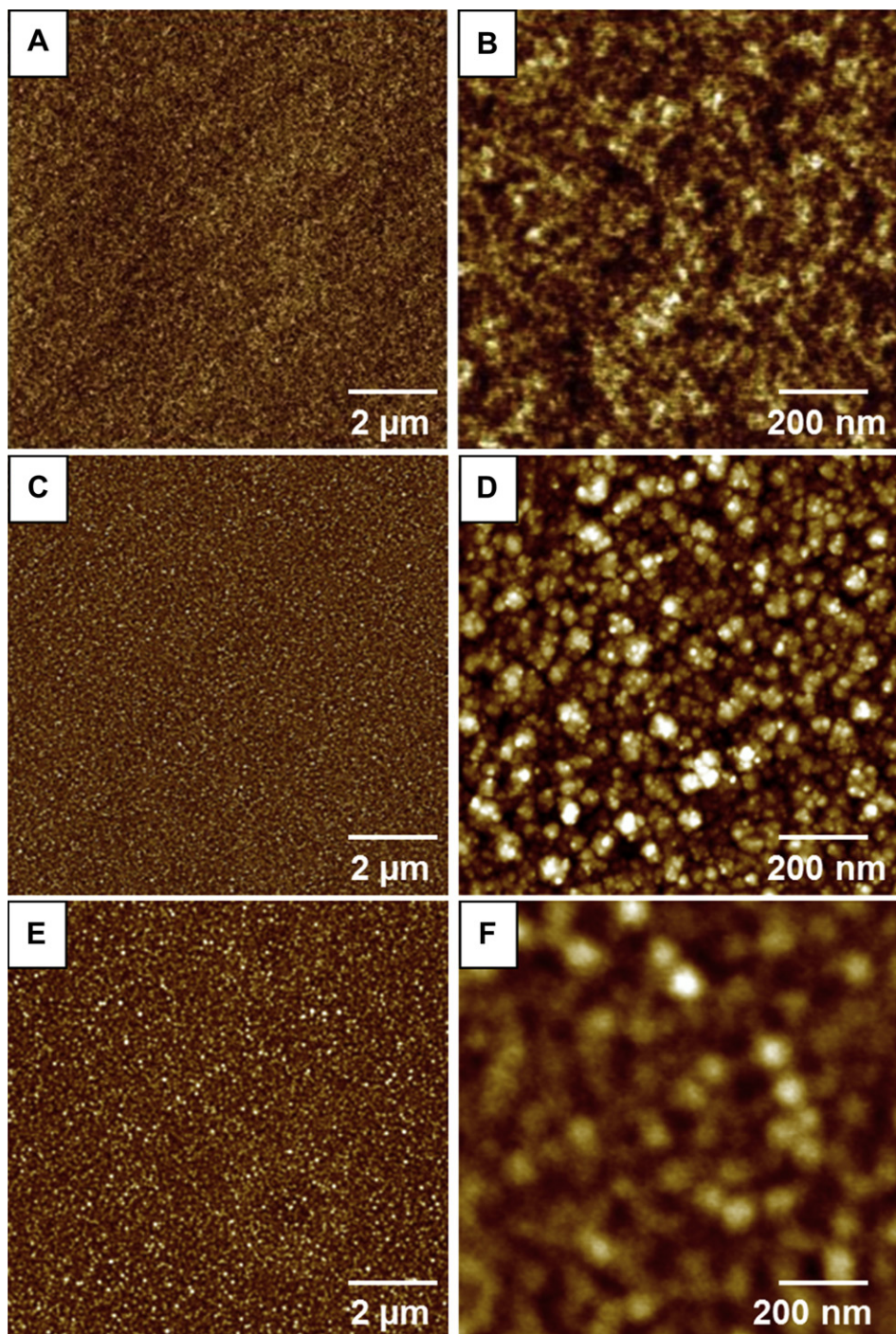


**Fig. 1.** AFM of A, B) PP-NIPAAm ( $Z = 2$  nm), C, D) PP-TTIP ( $Z = 16$  nm), E, F) PP-NIPAAm/TTIP ( $Z = 14$  nm) at low (left) and high (right) magnifications.

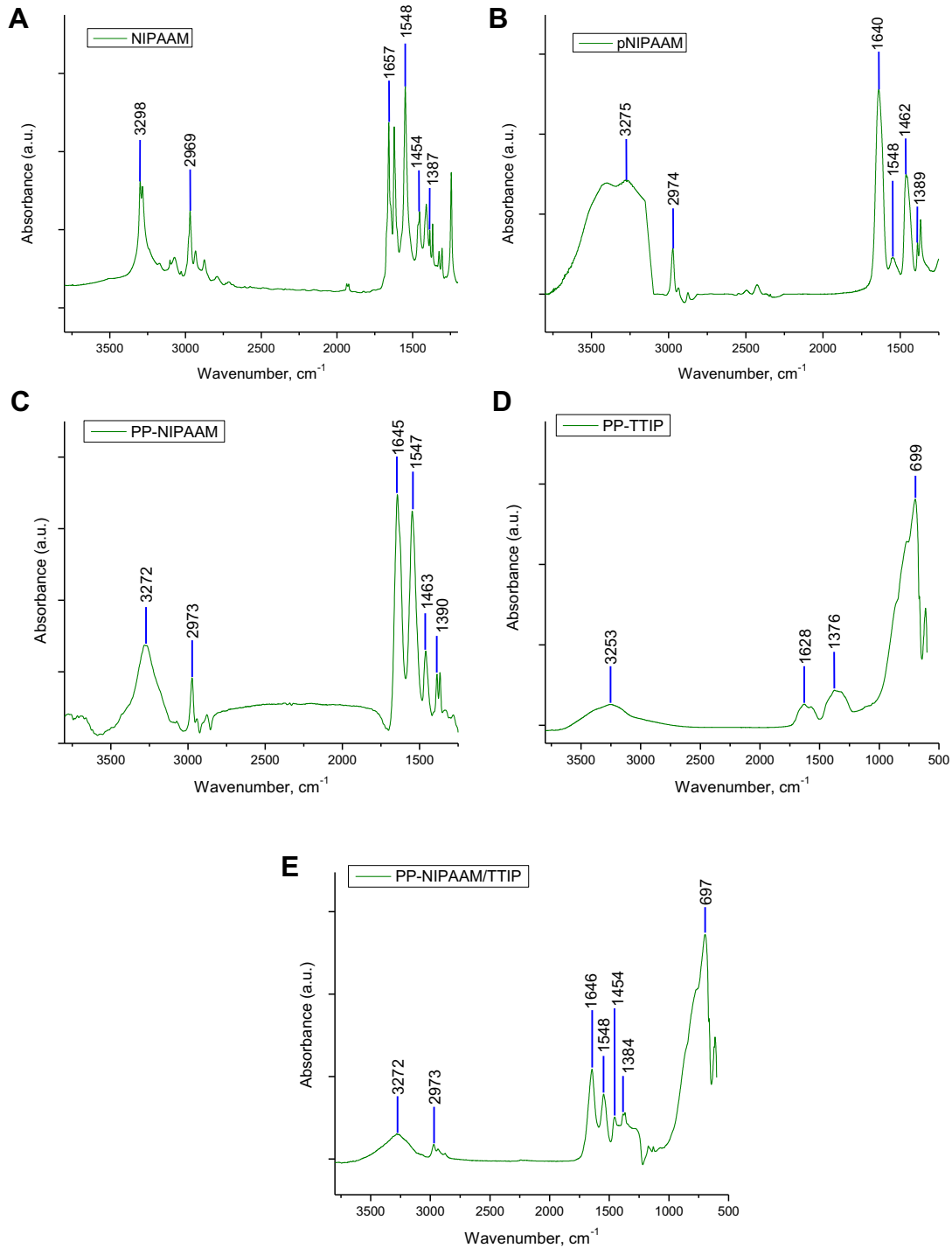


**Fig. 2.** FTIR spectra of A) NIPAAM monomer B) Spun-cast P-NIPAAM film and plasma polymerized films: C) PP-NIAAM, D) PP-TTIP and E) PP-NIPAAM/TTIP.

polymerized with the NIPAAM during initiated CVD. These films showed a similar response to other reports, providing further evidence that NIPAAM thin films can be used in rapid responsive microactuator or MEMS devices. Overall, these plasma polymerized films with relatively high crosslinking density show modest response in comparison with bulk gels [38]. Several recent studies have evaluated co-polymerization of distinct monomers for significant refractive index modification [39,40]. The addition of two or more monomers, each with a distinctive refractive index,

can be used as a method to create films with precisely tuned refractive indices set at a desired value [41,42]. Additionally, optical stacks have been fabricated which show remarkable tunability with a significant shift in reflectivity properties upon activation using swellable hydrogels sandwiched between high index layers [43].

Here, we demonstrate robust plasma polymerized single component films of NIPAAM and Titanium(IV) isopropoxide (TTIP) as well as corresponding robust composite films from these components. These

**Table 1**  
FTIR peak assignments for plasma polymerized films.

|                                     | NIPAAM | pNIP<br>AAM | PP-<br>NIPAAM | PP-TTIP | PP-NIPAAM/<br>TTIP |
|-------------------------------------|--------|-------------|---------------|---------|--------------------|
| N–H stretch                         | 3298   | 3275        | 3272          |         | 3272               |
| O–H stretch                         |        |             |               | 3252    |                    |
| C–H stretch                         | 2969   | 2974        | 2973          |         | 2973               |
| C=O stretch (amide I)               | 1657   | 1640        | 1645          |         | 1646               |
| C–C stretch                         | 1622   |             |               | 1628    |                    |
| N–H stretch (amide II)              | 1548   | 1548        | 1547          |         | 1548               |
| C–H symmetric bending               | 1454   | 1462        | 1463          |         | 1454               |
| C–CH <sub>3</sub> methyl bending I  | 1387   | 1389        | 1390          |         | 1384               |
| C–CH <sub>3</sub> methyl bending II | 1367   | 1368        | 1366          | 1376    |                    |
| Ti–O                                |        |             |               | 699     | 697                |

ultrathin composite films exhibiting a wide range of controllable refractive indices and, moreover, this refractive index responds significantly and reversibly to periodic environment humidity changes with much faster response time than that usually observed for traditional bulk one-component PNIPAAM films.

## 2. Experimental

### 2.1. Materials

All monomers, n-Isopropylacrylamide (97%) and titanium(IV) isopropoxide (99%) were purchased from Sigma–Aldrich and used as received for all subsequent plasma processes ([Scheme 1](#)). All plasma depositions were carried out on highly polished single crystal silicon substrates {100} (University Wafer) which were cleaned in piranha solution (*Caution! 3:1 concentrated H<sub>2</sub>SO<sub>4</sub> and 30% H<sub>2</sub>O<sub>2</sub>*). The wafers were then rinsed with Nanopure water (18 MΩ cm) following the standard accepted procedure [[44](#)]. pNIPAAM ( $M_w = 19,000\text{--}26,000$ ) was purchased from Sigma–Aldrich and dissolved in Nanopure water at a 2% concentration. The solution was then spin-cast on a clean silicon wafer at 3000 rpm for 30 s and used as a benchmark comparison against the plasma polymerized NIPAAM (PP-NIPAAM) films during FTIR measurements.

All plasma polymerization reactions were carried out using a custom built plasma flowing afterglow chamber with an argon or oxygen plasma at 13.56 MHz using a capacitively coupled RF power source according to established procedure [[45,46](#)]. The plasma was run under varying condition sets including 20–40 W powers, 0.1–0.2 Torr operating pressures, 20 sccm carrier gas flow rate and 5–9 min deposition times. Samples utilizing the TTIP monomer used an additional carrier gas of oxygen at a flow rate of 40–70 sccm filtered through the liquid monomer to assist with vaporization. The deposition times ranged from 2 to 10 min depending on the desired thickness of the final film. The solid NIPAAM monomer was placed directly into a sealed glass heating vessel and immersed in a water bath at 80 °C. This heating allowed the NIPAAM monomer to melt and vaporize into the plasma chamber when the flow valve was opened. The monomer inlet was downstream of the plasma-generating zone.

Careful control of the monomer flow was needed to ensure that the flow rate was kept low so that excessively fast film depositions would not occur. It was observed that films deposited under very high deposition rates (>100 nm/min) lead to films that were unstable and typically delaminated from the surface due to internal stresses. The TTIP monomer was placed in a custom-built bubbling apparatus for vaporization and heated to 60 °C in a water bath. The tubing connecting the bubbler to the plasma chamber was also heated to prevent condensation of the monomer before entering the plasma chamber. After plasma polymerization, the films were removed from the chamber and stored under normal atmosphere

for a minimum of 48 h before further testing was carried out to allow any residual internal stresses in the films to equilibrate.

### 2.2. Characterization

Atomic force microscopy (AFM) imaging was performed on a Bruker Icon system with a Nanoscope V controller in air. Triangular shaped ScanAsyst-Air cantilevers (Bruker) with a nominal spring constant of 0.4 N/m were used for all scans. Scan sizes from 10 μm to 400 nm were collected in the PeakForce® mode. All surface roughness measurements were averaged over six 1 × 1 μm [[2](#)] areas in several locations [[47](#)]

Thickness, optical property, and film responsiveness measurements were conducted using an M-2000U (Woollam Co) variable angle spectroscopic ellipsometer ( $\lambda = 250\text{--}1000$  nm). Thickness and optical properties were measured at 65°, 70° and 75° and the data was fit using the B-Spline model in the CompleteEASE software package. Focusing ring attachments were included in the ellipsometer set up to more accurately focus the probing light beam at a desired location. A Peltier heating stage was placed under the sample and the temperature was controlled during response testing. A liquid cell was placed over the top of the sample to contain the moisture. All measurements with the fluid cell were carried out at a 70° angle as the liquid cell was fixed. Connection ports on the fluid cell allowed dry and wet nitrogen to be exposed to the films. Water vapor was added to dry nitrogen by bubbling it through a water bath and then directing it to the film surface for testing. Continuous dynamic scans were captured using the ellipsometer as the gas inlet lines were switched.

The swelling of the PP-NIPAAM film during moisture exposure was measured with quartz micro balance at a Masscal G1 controlled environment system. Films were plasma deposited directly onto quartz disks and placed in the sealed chamber at 25 °C. The inlet of dry and wet nitrogen was controlled using mass flow controllers at rates from 10 to 50 sccm. The measurement system consisted of a QCM enclosed in a temperature controlled chamber with a sealed cap around the sample which precisely controlled the atmosphere. The flow rates of dry and moist nitrogen were controlled using mass flow controllers with pre-programmed settings to allow increasing amounts of moist air into the chamber after a brief recovery period in which only dry nitrogen was purged to return the polymerized film to its original state.

Fourier transform infrared (FTIR) spectroscopy measurements were performed using a Bruker FTIR spectrometer (Vertex 70) equipped with a narrow-band mercury cadmium telluride detector in reflection mode. Spectra were collected for each sample from 4000 to 500 cm<sup>-1</sup> at intervals of 1 cm<sup>-1</sup> steps and averaged over 16 scans. Surface composition was obtained via X-ray photoelectron spectroscopy (XPS) using a Thermo K-Alpha XPS system with an Al K $\alpha$  source and utilizing charge neutralization. Survey spectra were collected over the range of 0–1000 at 1 eV steps with a spot size of 250 μm averaged over two scans. High resolution scans were performed in the range of relevance for specific elements at 0.1 eV steps and averaged over five scans. A depth profile of the sample was done by etching 10 layers for a duration of 10 s each at 2000 eV. The approximate etching rate was 1.8 nm/s, as estimated from a Ta<sub>2</sub>O<sub>5</sub> standard.

## 3. Results and discussion

### 3.1. Surface morphology

Large scale AFM images of PP-NIPAAM films show uniform surface coverage at different length scales with no visible pinholes defects ([Fig. 1A](#)). Corresponding high resolution AFM imaging of the PP-NIPAAM film shows a fine grainy morphology with a very low surface roughness ([Fig. 1B](#)). The surface microroughness measured

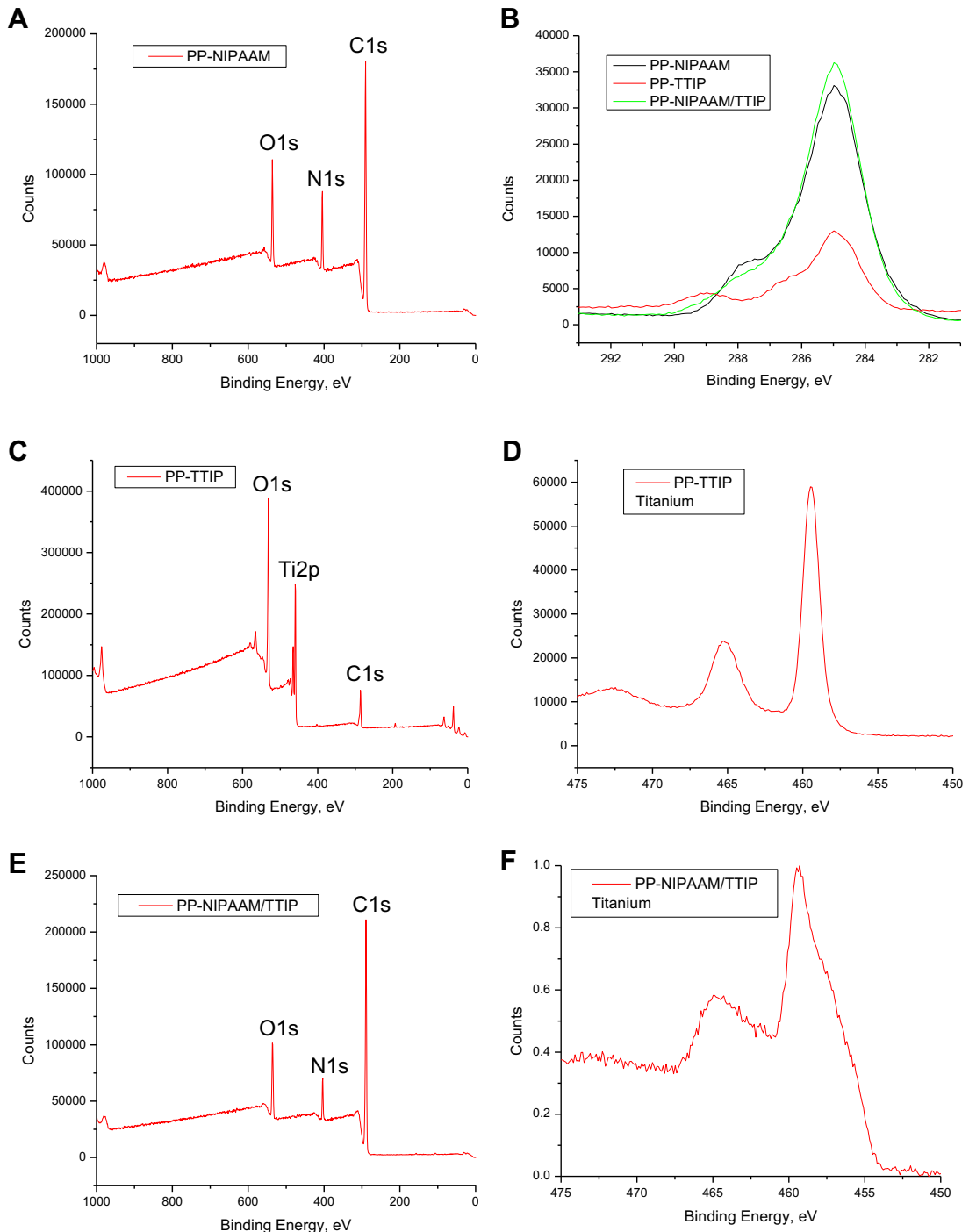


**Fig. 3.** XPS of A) PP-NIPAAM film, B) High resolution carbon signal of all three materials. C) PP-TTIP, D) High resolution of the titanium signal from the PP-TTIP film. E) PP-NIPAAM/TTIP and F) High resolution of the titanium signal from the PP-NIPAAM/TTIP film after film etching.

within a  $1 \times 1 \mu\text{m}$  [2] surface area was very low, below 0.4 nm which is common for uniform one-component plasma polymerized films with smooth local morphology [27,30,31].

The PP-TTIP film exhibited many fine, round features which leads to much rougher surface ( $\sim 2.6$  nm) which is readily apparent at higher magnifications on AFM (Fig. 1C and D). The surface roughness of the PP-TTIP film varies based within a narrow window on the atmosphere of the plasma chamber. Our studies showed that the argon atmosphere used with many materials leads to a lower surface roughness of the PP-TTIP film as well as a lower refractive index. For this reason, an oxygen atmosphere was used to promote

oxidation of the TTIP monomer, thus forming a higher refractive index film. Previous studies have detailed the use of different deposition atmospheres with titania precursors and found that oxygen rich atmospheres typically allow for more complete oxidation to the  $\text{Ti}^{4+}$  state and promotes the most complete conversion of the precursor to titania versus an argon atmosphere as well as the formation of carbon bonding from the methyl groups in the monomer [48,49].

AFM images of the composite thin film show a surface morphology exhibiting features of both (Fig. 1E). The film appears to be uniform and free of major defects, indicating the plasma

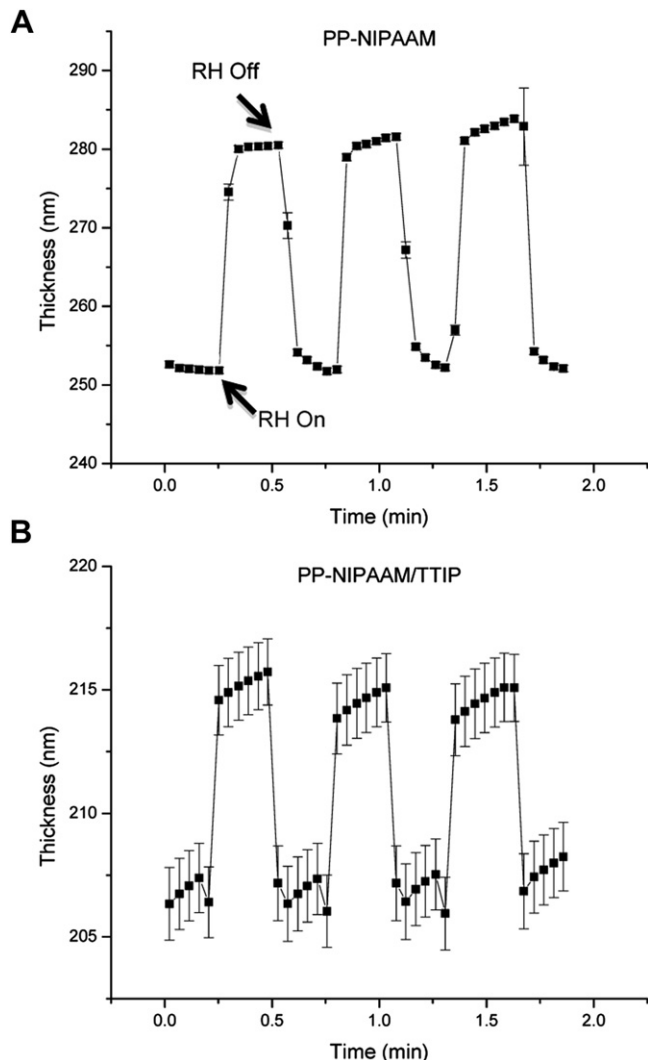


Fig. 4. Thickness variation at on/off moisture cycling for films: A) PP-NIPAAm and B) PP-NIPAAm/TTIP.

deposition process uniformly coats the substrate surface. Higher magnification reveals some nodes and nanoscale features are visible on the surface. These features are similar to, but are not as distinct as the pure PP-TTIP film. Compared to the PP-TTIP film these features are “blurred” due to coverage with the PP-NIPAAm component. The fine surface structure seen in the PP-NIPAAm film is not visible on the co-polymerized surface as a result of the monomers co-polymerizing. The surface microroughness of 1.8 nm within a  $1 \times 1 \mu\text{m}$  [2] surface area is lower than that for the single component TTIP film that reflects the smoothening due to the presence of the polymer in addition to inorganic component.

### 3.2. Chemical composition: FTIR & XPS analysis

The FTIR peak assignments for PP-NIPAAm include the N–H (secondary amide) stretch at  $3272 \text{ cm}^{-1}$ , C–H asymmetric stretch at  $2973 \text{ cm}^{-1}$ , C=O (amide I) stretch at  $1645 \text{ cm}^{-1}$ , N–H (amide II) stretch at  $1548 \text{ cm}^{-1}$ , C–H bending at  $1463 \text{ cm}^{-1}$  and two final peaks at  $1390 \text{ cm}^{-1}$  and  $1366 \text{ cm}^{-1}$  which are indicative of the methyl groups in the NIPAAm structure (Fig. 2, Table 1). The retention of these groups is important, as it is believed that they are contributors to the phase transition in the PP-NIPAAm film [12].

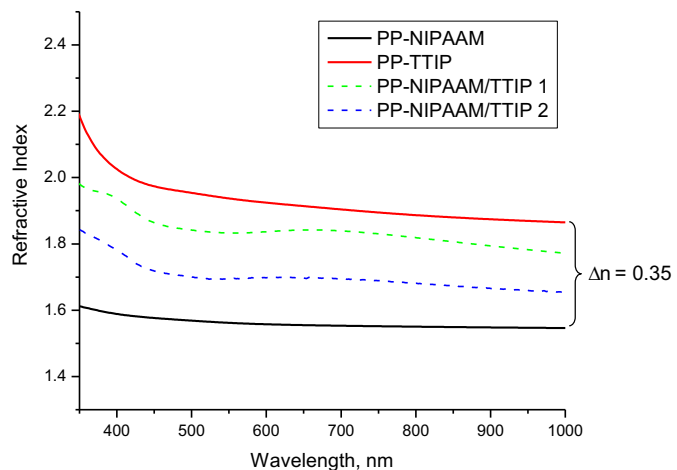


Fig. 5. Refractive index of PP-NIPAAm, PP-TTIP and PP-NIPAAm/TTIP (two different compositions) films.

The same peaks are seen in the spun-cast pNIPAAm film providing direct verification a polymerization reaction is occurring during the deposition although to a great extent the initial chemical composition and bonding is retained [10,12,29]. The spectra suggest that the monomers are not undergoing complete dissociation, a desirable feature of low-power plasma deposition.

The expected peaks of Ti–O at  $699 \text{ cm}^{-1}$ , residual carbon bonding ( $1628 \text{ cm}^{-1}$ ), and methyl groups ( $1376 \text{ cm}^{-1}$ ) are seen in the PP-TTIP film [50]. The co-polymerized PP-NIPAAm/TTIP film shows distinguishing characteristics of both materials with a Ti–O peak at  $697 \text{ cm}^{-1}$  and the characteristic peaks of PP-NIPAAm at  $1646 \text{ cm}^{-1}$ ,  $1548 \text{ cm}^{-1}$ ,  $1454 \text{ cm}^{-1}$  and  $1384 \text{ cm}^{-1}$  (Fig. 2). Some broadening of these peaks is seen in comparison to the pure PP-NIPAAm film. Excess carbon and carbon bonding may be seen in the co-polymer spectra since there is the potential for residual methyl groups of the TTIP monomers to bond to the surface. Overall, the FTIR spectra indicate that the monomers are not undergoing significant dissociation by the plasma and are only radicalized to become reactive. The term “co-polymerization” which is used here does not necessarily refer to the fact that the monomers form a defined co-polymer chemical structure in the traditional sense; rather they are polymerized under the same conditions at the same time thus, possibly, forming random interpenetrating network. It is entirely possible that the form some type of complex, but the structure of plasma polymerized films is a subject of debate and we do not have a conclusive way to definitively strictly-defined chemical structures are produced in the film.

XPS analysis of all plasma-polymerized films verifies the expected compositions, which correspond directly to the chemical structures of the polymer (Fig. 3). High resolution XPS of the carbon content of all three films showed an expected C–C and C–H bonding referenced at 285 eV [29]. The PP-NIPAAm spectrum showed the expected presence of a carbonyl group (C=O) at 287.7 eV. This peak was also seen in the PP-TTIP film at 288.9 eV and through deconvolution of the PP-NIPAAm/TTIP film at 287.6 eV, as expected in these films (Figure S1). As the two materials are co-polymerized this peak shifts closer to that of the PP-NIPAAm due to the increasing number of carbonyl groups of NIPAAm origin present on the surface.

The PP-NIPAAm spectrum shows strong carbon, oxygen and nitrogen peaks and PP-TTIP spectrum shows the expected titanium, oxygen and residual carbon peaks, which results from the methyl groups attached to the titanium atom in the monomer. Under appropriate conditions these excess groups will form an

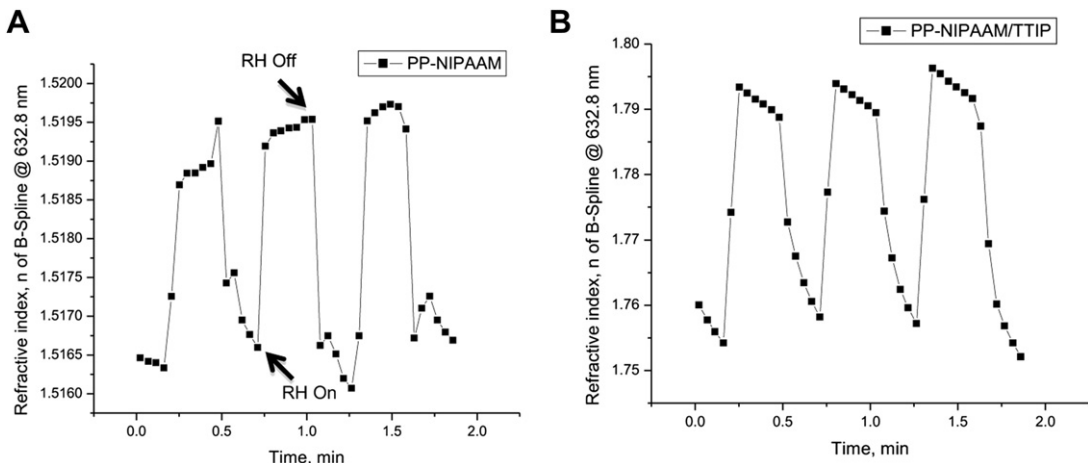


Fig. 6. Changing refractive index values through relative humidity cycling for A) PP-NIPAAm and B) PP-NIPAAm/TTIP.

independent carbon containing system on the surface as well [48]. The copolymerized film also shows the characteristic peaks of carbon, oxygen and nitrogen, but the surface scan does not reveal the presence of titanium (Fig. 3E). XPS surface scans typically only penetrate approximately the first 10 nm of the film and thus only reveal the surface composition. Upon etching of the film however, a titanium signal emerges and becomes very distinct after ten etch cycles (Fig. 3E and F). This result indicates that there is a carbon rich capping layer covering the composite films as has been suggested above based upon more uniform surface morphology. This excess carbon layer might likely occur from carbon contamination on the surface after it is removed from the vacuum chamber. On the other hand, different rates of reaction and different wettability of polymer and inorganic monomers might also result in the polymer component saturating the topmost layer.

### 3.3. Film response

Nominal thickness values of all films tested were around 200 nm as measured via ellipsometry and SEM (Figure S2). The PP-TTIP films and a bare substrate were characterized in the same manner as the PP-NIPAAm films with moisture cycling between dry and high humidity nitrogen to account for moisture collection on control surfaces (not shown). Very little changes, close to the sensitivity limit (about 1 nm), were seen in all cases (see SI).

PP-NIPAAm films exhibit an easily measurable thickness response when exposed to higher humidity similar to those observed for PP-NIPAAm films in water [12,33,34]. The high humidity atmosphere causes swelling in the film as the PP-NIPAAm film absorbs water in its hydrophilic state below the LCST as compared to higher temperatures where swelling is much less pronounced (Fig. 4A). The fast response shown (few seconds) was obtained through the rapid switching between a dry (1.5% relative humidity) and water saturated nitrogen (95% relative humidity) atmosphere that was directly exposed to the film while it was on the ellipsometer stage under a continuous, dynamic measuring regime, which collected measurements at regular intervals. Both single, long moisture exposure and short, rapid switching regimes are demonstrated indicating multiple consistent cycling was observed (Figure S3).

A response at 25 °C of between 16 and 20 nm (12% film thickness) and a response time of about 2 s was observed. This swelling ratio is smaller than traditional swollen hydrogel systems due to the higher expected crosslink densities of plasma polymerized films. UV-grafted PNIPAAm examples from literature showed similar response times

but significantly larger swelling ratios given their lower crosslinking [7]. The single transition profiles indicate that long time exposure to moisture, the transition in thickness is still rapid and stable at both high and low humidity conditions (Figure S3).

The copolymerized PP-NIPAAm/TTIP film response was similar overall to that of the PP-NIPAAm film (Fig. 4B). Even with the addition of the non-responsive titanium dioxide material, the PP-NIPAAm/TTIP films exhibit a response to the humidity albeit a smaller percentage. These tests were repeated using much shorter on/off cycle times for the moisture exposure. Each sample continued to show similar response behavior after repeated mounting and moisture exposure. The swelling time in which the thickness change occurred was between one and 2 s. More precise transition time measurements were limited by the time required between measurements on the ellipsometer.

### 3.4. Tailored refractive index

The measured values are 1.95 for PP-TTIP film and 1.6 for PP-NIPAAm (Fig. 5). This combination thus allows a potential refractive index range of 0.35 at extreme compositions to be expected. The co-polymerized film indeed shows a refractive index consistent between the two refractive index values (Fig. 5). By adjusting the deposition ratios of the monomers, the resulting refractive index of the composite film was varied within the designated range (see two examples in Fig. 5). Several recent studies have evaluated copolymerization of distinct monomers for significant refractive index modification [39,40]. The addition of two or more monomers, each with a distinctive refractive index, can be used as a method to create films with precisely tuned refractive indices set at a desired value [51–53].

Thus, the co-polymerization of these two monomers (NIPAAm and TTIP) provides a facile method of creating a robust ultrathin coating with a higher refractive index than that of a pure polymer, while still retaining some of the moisture responsiveness seen in the pure PP-NIPAAm films as the thickness changes. Such a film could find potential use in many optical applications, especially detection and responsive scenarios. Higher index layers with PP-TTIP may be possible at higher temperatures as suggested in literature which detail the formation of anatase phase from TTIP precursor deposited at 300 °C [54]. Lower temperature depositions are necessary in this case to preserve the polymer and most likely result in amorphous titania being formed. The optical absorption of all three films (PP-NIPAAm, PP-TTIP and PP-NIPAAm/TTIP) is very low, below 0.04 over the visible range for each of the materials,

making these types of films ideal for application where optical transmission is of importance.

### 3.5. Tunable refractive index

A small but detectable repeatable change in the refractive index ( $\sim 0.01$ ) during the moisture exposure was observed typically in the PP-NIPAAAM films (Fig. 6). The change in the index was typically much higher as expected, around 0.03, for the copolymerized film. The refractive index change occurs quickly, remains stable for the duration of the applied conditions and then returns to the initial state. The transition from low to high index occurred in less than 2 s, as with the thickness changes. This type of rapid cycling demonstrates the fast, reversible nature of the films and how this can be applied in applications where refractive index adjustments are of interest. By composing the film with a specific index from the mixture of the two monomers, tunable films can be applied over a wide range of refractive indices. These changes corresponded to the thickness changes of the film and the baseline refractive index can be adjusted to various levels by controlling the ratio of each monomer in the film.

## 4. Conclusions

In conclusion, we demonstrated that PP-NIPAAAM films fabricated using plasma enhanced chemical vapor deposition techniques respond rapidly to changes in humidity as observed through thickness and refractive index measurements. Relative humidity change is an effective trigger for rapid (few seconds) switching which is order of magnitude faster than that usually observed for bulk PNIPAAAM films. Co-polymerization of reactive NIPAAAM monomer with an inorganic-based precursor, TTIP allows for ultrathin composite films with varying degrees of responsiveness as well as final optical properties. A significant variation of the refractive index can also be observed during the humidity exposure experiments. This type of switching can be used in photonic applications requiring defined, high refractive indices while still exhibiting a response. The film responds with a change in thickness and refractive index at very low amounts of moisture, which would allow such a system to be used in highly sensitive optical systems, where tunable optical properties are desirable. The design of the materials is a key factor in tailoring the responsiveness of the film to meet specific system design requirements. Reversible switching of the thickness and refractive index of composite films is a practical demonstration of a use of these types of responsive ultrathin films, which can be tailored to specific, responsive photonic or sensing applications.

## Acknowledgments

This work was supported by the Department of Defense (DoD) through the National Defense Science & Engineering Graduate Fellowship (NDSEG) program. This research is also supported by the Air Force Office of Scientific Research FA9550-08-1-0446 and FA9550-09-1-0162, as well as the Air Force Research Lab. The authors thank Seth Young for technical assistance with FTIR measurements.

## Appendix A. Supplementary material

Supplementary material associated with this article can be found, in the online version, at <http://dx.doi.org/10.1016/j.polymer.2012.08.013>

## References

- [1] White TJ, Tabiryan NV, Serak SV, Hrozyk UA, Tondiglia VP, Koerner H, et al. *Soft Matter* 2008;4:1796–8.
- [2] Schmidt S, Motschman H, Hellweg T, von Klitzing R. *Polymer* 2008;49:749–56.
- [3] Juthongpuit D, Lin Y-H, Teng J, Zubarev ER, Tsukruk VV. *J Am Chem Soc* 2003;125:15912–21.
- [4] Kang Y, Walish JJ, Gorishnyy T, Thomas EL. *Nat Mater* 2007;6:957–60.
- [5] Peleshanko S, Anderson KD, Goodman M, Determan MD, Mallapragada SK, Tsukruk VV. *Langmuir* 2007;23:25–30.
- [6] Stuart MAC, Huck WTS, Genzer J, Mueller M, Ober C, Stamm M, et al. *Nat Mater* 2010;9:101–13.
- [7] Xu W, Yin X, He G, Zhao J, Wang H. *Soft Matter* 2012;8:3105–11.
- [8] Luzinov I, Minko S, Tsukruk VV. *Prog Polym Sci* 2004;29:635–98.
- [9] Jones DM, Smith JR, Huck WTS, Alexander C. *Adv Mater* 2002;14:1130–4.
- [10] Tu H, Heitzman CE, Braun PV. *Langmuir* 2004;20:8313–20.
- [11] Harmon ME, Kuckling D, Frank CW. *Langmuir* 2003;19:10660–5.
- [12] Pan YV, Wesley RA, Luginbuhl R, Denton DD, Ratner BD. *Biomacromolecules* 2001;2:32–6.
- [13] Matsukuma D, Yamamoto K, Aoyagi T. *Langmuir* 2006;22:5911–5.
- [14] Bucio E, Burillo G, Adem E, Coqueret X. *Macromol Mater Eng* 2005;290:745–52.
- [15] Alf ME, Hatton TA, Gleason KK. *Thin Solid Films* 2011;519:4412–4.
- [16] Alf ME, Godfrin PD, Hatton TA, Gleason KK. *Macromol Rapid Commun* 2010;31:2166–72.
- [17] LeMieux MC, Peleshanko S, Anderson KD, Tsukruk VV. *Langmuir* 2007;23:265–73.
- [18] Canavan HE, Cheng X, Graham DJ, Ratner BD, Castner DG. *Langmuir* 2005;21:1949–55.
- [19] Jiang X, Bai J, Gittens SA, Uludağ H. *Mat-wiss U Werkstofftech* 2006;37:462–8.
- [20] Delcea M, Schmidt S, Palankar R, Fernandes PAL, Fery A, Möhwald H, et al. *Small* 2010;6:2858–62.
- [21] Hess DW. *J Vac Sci Technol A* 1990;8:1677–84.
- [22] Förch R, Chifén AN, Bouquet A, Khor HL, Jungblut M, Chu L-Q, et al. *Chem Vapor Depos* 2007;13:280–94.
- [23] Sreenivasan R, Gleason KK. *Chem Vap Deposition* 2009;15:77–90.
- [24] Tenhaeff W, Gleason KK. *Adv Funct Mater* 2008;18:979–92.
- [25] Alf ME, Asatekin A, Barr MC, Baxamusa SH, Chelawat H, Ozaydin-Ince G, et al. *Adv Mater* 2010;22:1993–2007.
- [26] Im SG, Gleason KK. *AIChE J* 2011;57:276–85.
- [27] Anderson KD, Luo M, Jakubiak R, Naik RR, Bunning TJ, Tsukruk VV. *Chem Mater* 2010;22:3259–64.
- [28] Singamaneni S, LeMieux MC, Lang HP, Gerber Ch, Lam Y, Zauscher S, et al. *Adv Mater* 2008;20:653–80.
- [29] Teare DOH, Barwick DC, Schofield WCE, Garrod RP, Beeby A, Badyal JPS. *J Phys Chem B* 2005;109:22407–12.
- [30] Anderson KD, Slocik JM, McConney ME, Enlow JO, Jakubiak R, Bunning TJ, et al. *Small* 2009;5:741–9.
- [31] Anderson KD, Marczewski K, Singamaneni S, Slocik JM, Naik RR, Bunning TJ, et al. *ACS Appl Mater Inter* 2010;2:2269–81.
- [32] Lee YM, Shim JK. *Polymer* 1997;38:1227–32.
- [33] Tamirisa PA, Hess DW. *Macromolecules* 2006;39:7092–7.
- [34] Tamirisa PA, Koskinen J, Hess DW. *Thin Solid Films* 2006;515:2618–24.
- [35] Yagüe JL, Gleason KK. *Soft Matter* 2012;8:2890–4.
- [36] Cheng X, Canavan HE, Stein MJ, Hull JR, Kweskin SJ, Wagner MS, et al. *Langmuir* 2005;21:7833–41.
- [37] Alf ME, Hatton TA, Gleason KK. *Polymer* 2011;52:4429–34.
- [38] Tokarev I, Minko S. *Soft Matter* 2009;5:511–24.
- [39] Jiang H, Grant JT, Tullis S, Eyink K, Fleitz P, Bunning TJ. *Polymer* 2004;45:8475–83.
- [40] Jiang H, Grant JT, Eyink K, Tullis S, Enlow J, Bunning TJ. *Polymer* 2005;46:8178–84.
- [41] Jiang H, O'Neill K, Grant JT, Tullis S, Eyink K, Johnson WE, et al. *Chem Mater* 2004;16:1292–7.
- [42] Anderson KD, Young SL, Jiang H, Jakubiak R, Bunning TJ, Naik RR, et al. *Langmuir* 2012;28:1833–45.
- [43] Karaman M, Kooi SE, Gleason KK. *Chem Mater* 2008;20:2262–7.
- [44] Tsukruk VV, Bliznyuk VN. *Langmuir* 1998;14:446–55.
- [45] Jiang H, Johnson WE, Grant JT, Eyink K, Johnson EM, Tomlin DW, et al. *Chem Mater* 2003;15:340–7.
- [46] Enlow JO, Jiang H, Grant JT, Eyink K, Su W, Bunning TJ. *Polymer* 2008;49:4042–5.
- [47] McConney ME, Singamaneni S, Tsukruk VV. *Polym Rev* 2010;50:235–86.
- [48] Ahn K-H, Park Y-B, Park D-W. *Surf Coat Technol* 2003;17:198–204.
- [49] Fictorie CP, Evans JF, Gladfelter WL. *J Vac Sci Technol A* 1994;12:1108–13.
- [50] Hernandez-Perez MA, Garapon C, Champeaux C, Orlanges JC. *J Phys Conf Ser* 2007;59:724–7.
- [51] Jiang H, O'Neill K, Grant JT, Tullis S, Eyink K, Johnson WE, Fleitz P, Bunning TJ. *Chem Mater* 2004;16:1292–7.
- [52] Anderson KD, Young SL, Jiang H, Jakubiak R, Bunning TJ, Naik RR, Tsukruk VV. *Langmuir* 2012;28:1833–45.
- [53] Peri SR, Kim H, Akgun B, Enlow J, Jiang H, Bunning TJ, et al. *Polymer* 2010;51:3971–7.
- [54] Niskanen A, Arstila K, Leskelä M, Ritala M. *Chem Vap Deposition* 2007;13:152–7.